PERGAMON

International Journal of Heat and Mass Transfer 44 (2001) 827–836

International Journal of HEAT and MASS TRANSFER

www.elsevier.com/locate/ijhmt

On the effective thermal conductivity of a three-dimensionally structured fluid-saturated metal foam

K. Boomsma, D. Poulikakos*

Laboratory of Thermodynamics in Emerging Technologies, Institute of Energy Technology, Swiss Federal Institute of Technology, ETH Center, 8092 Zurich, Switzerland

Received 12 January 2000; received in revised form 15 March 2000

Abstract

A geometrical effective thermal conductivity model of a saturated porous metal foam was developed, based on the idealized three-dimensional basic cell geometry of a foam, the tetrakaidecahedron. This geometric shape results from filling a given space with cells of equal size yielding minimal surface energy [1]. The foam structure was represented with cylindrical ligaments which attach to cubic nodes at their centers. The relative geometrical lengths were calibrated with experiments [2]. It was found that the model estimated the effective thermal conductivity very well for these experimental configurations. It was shown that changing the fluid conductivity has a relatively small effect on increasing the effective thermal conductivity. For an aluminum foam (k = 218 W m^{-1} K^{-1}) with 95% porosity in vacuum, the three-dimensional model predicted a k_{eff} of 3.82 W m^{-1} K^{-1}. Using air as the saturating fluid (k = 0.0265 W m^{-1} K^{-1}) increased the thermal conductivity to 3.85 W m^{-1} K^{-1}, and water (k = 0.613 W m^{-1} K^{-1}) increased the thermal conductivity to 4.69 W m^{-1} K^{-1}. This shows that despite the high porosity of the foam, the heat conductivity of the solid phase controls the overall effective thermal conductivity to a large extent, a fact that must be dealt with in the foam manufacturing process if specific ranges of the foam effective conductivity are desired. It also implies that an accurate representation of the contribution of the solid portion of the foam to the effective thermal conductivity is needed in effective conductivity models. Detailed expressions for the foam effective thermal conductivity were derived in the course of this work and are reported in this paper. © 2001 Published by Elsevier Science Ltd.

Keywords: Conduction; Heat exchangers; Porous media

1. Introduction

Analytical approximations for the effective thermal conductivity in a stagnant fluid flow condition in one direction has been sought ever since the first investigations in the field of porous media by Maxwell [3] and Lord Rayleigh [4]. The value of the effective thermal conductivity of porous media proves to be useful in heat transfer applications ranging from soil and gravel layers, to foam insulation, and recently, to the novel application of open celled metal foam heat exchangers, which constitutes the focus of this work. The complexity of the geometry encountered in the foam, along with the large difference in thermal con-

* Corresponding author. Tel.: +41-1-6322738; fax: +41-1-6321176.

E-mail address: poulikakos@ltnt.iet.mavt.ethz.ch (D. Poulikakos).

0017-9310/01/$ - see front matter © 2001 Published by Elsevier Science Ltd.
PII: S0017-9310(00)00123-X

Nomenclature

a	foam ligament radius (m)
d	dimensionless foam ligament radius
e	dimensionless cubic node length
k	thermal conductivity (W m^{-1} K^{-1})
L	ligament length (m)
R	simplification quantity (W^{-1} m K)
r	cubic node length (m)
V	volume (m^3)

Subscripts

A	unit cell subsection
B	unit cell subsection
C	unit cell subsection
D	unit cell subsection
eff	effective
f	fluid
n	A, B, C, D
s	solid

Greek symbol

ε	porosity

ductivity between the fluid and solid phases, present a challenge in approximating the heat transfer coefficient compared to previous work done mainly with particles in a packed bed [5–8].

The value of the thermal conductivity in the solid–fluid composite is required in the numerical modeling of forced convection through porous media [7]. Hunt and Tien [9] used an empirical stagnant conduction model developed by Tien and Vafai [10] to define the effective thermal conductivity in the volume averaged homogeneous energy equation. Antohe et al. [11] also required the use of an empirical phase symmetry conduction that was developed by Hsu et al. [12] to create a numerical model for the simulation of cooling micro heat exchangers. The origins of the phase-symmetry conduction model by Hsu et al. [12] are based upon the original work done by Zehner and Schlunder on packed beds of spheres [13].

A first order estimate of the effective thermal conductivity of a fluid filled porous media can be made by simply accounting for the volume fraction of each substance, giving the resulting relation based on the porosity and the thermal conductivity of each substance.

$$k_{\text{eff}} = \varepsilon k_{\text{f}} + (1-\varepsilon)k_{\text{s}} \tag{1}$$

This equation, however, does not account for natural convection between the solid to the fluid phases, contact resistance between packed particles or cells, radiation, or distinct structural features. The stagnant models that have been previously developed required some additional assumptions concerning the behavior of the heat flow through the composite medium and the porous medium itself. These include:

1. The porous medium is uniform, or the porosity variation can be accurately calculated.
2. Natural convection and radiation heat transfer effects inside the porous medium can be neglected.
3. The physical properties of the solid and fluid phases remain constant throughout the temperature range.
4. The solid and fluid phases are in local thermal equilibrium.

Assumption No. 4 is a pivotal measure that is taken to enable one energy equation to be used later in the volume averaging technique utilized in the numerical studies of the forced convection cases [14]. This actually allows a very small temperature difference between the two phases, or equivalently, comparable local temperature gradients [15]. Amiri and Vafai [16] have performed an extensive study into the validity of the local thermal equilibrium assumption. They found that the quality of this assumption for a packed bed of spheres diminished as the Darcy number and the particle Reynolds number increased. In other words, the local thermal equilibrium assumption works best, as perhaps expected, with slow moving or stagnant flows which are commonly found in porous media with relatively low permeabilities.

In a configuration with a low solid volume fraction and order of magnitude differences between the thermal conductivities of the two phases, the key in estimating the effective thermal conductivity is an accurate description of the geometry of the solid medium [17]. This technique was done successfully for a packed bed of spheres by Zehner and Schlunder [13]. They defined a unit cell consisting of one eighth of a cube centered around a solid sphere with the edge length equal to half the distance between the centers of the spheres. They assumed heat conduction in one dimension along two parallel paths; one path is the outer concentric cylinder and the other is the inner cylinder. The inner cylinder has a diameter equal to the diameter of the spherical particle and is composed of both fluid and solid, while the outer cylinder is purely fluid.

A recent advancement in the estimation of the effective thermal conductivity specifically for a metallic foam saturated with a fluid utilizing a geometrical esti-

mate was developed by Calmidi and Mahajan [2]. In this work, a basic, two-dimensional structure of a metallic foam was modeled by a hexagonal honeycomb shape using squares as the geometrical representation of the nodes. In the honeycomb shape, the thickness and length of the ligaments joining the nodes were adjustable, in addition to the length of the edge of the square node. In a representative cell section, distinct layers in the vertical (heat conducting) direction were defined based on characteristics of the geometry. The effective thermal conductivity was determined for each geometrical section directly through a macroscopic volume averaging procedure based on the porosity, similar to that, which yielded Eq. (1). After the thermal conductivity was obtained for each layer, the overall effective thermal conductivity for the representative unit cell was calculated by summing the layer resistances in series. To accurately represent the true effective thermal conductivity, the equation had to be calibrated through experimentation to determine the relative length and thickness of the ligaments to the size of the square nodes.

Based on the encouraging results of such a two-dimensional conduction model, as well as on the fact that an accurate representation of the metal foam geometry is of importance for the estimation of the effective thermal conductivity, we extend in this paper the idea of one-dimensional heat conduction in a two-dimensional foam structure [2] to the markedly more complex three-dimensional structure, which real metal foams possess. This is the incentive behind the present work. After the determination of a three-dimensional foam representation, the effective heat transfer coefficient of the saturated solid was obtained by a detailed layer-averaging scheme that is a three-dimensional generalization of that of Calmidi and Mahajan [2].

2. Foam geometry

The first task required that the foam geometry in three dimensions be well defined. This problem entails describing the space filling arrangement of cells of equal size with the minimal surface energy. The structure that accomplishes this, which has been accepted for the past 100 years is that of the tetrakaidecahedron (Fig. 1a). This complete cell which consists of six squares and eight hexagons was first published in Phi-

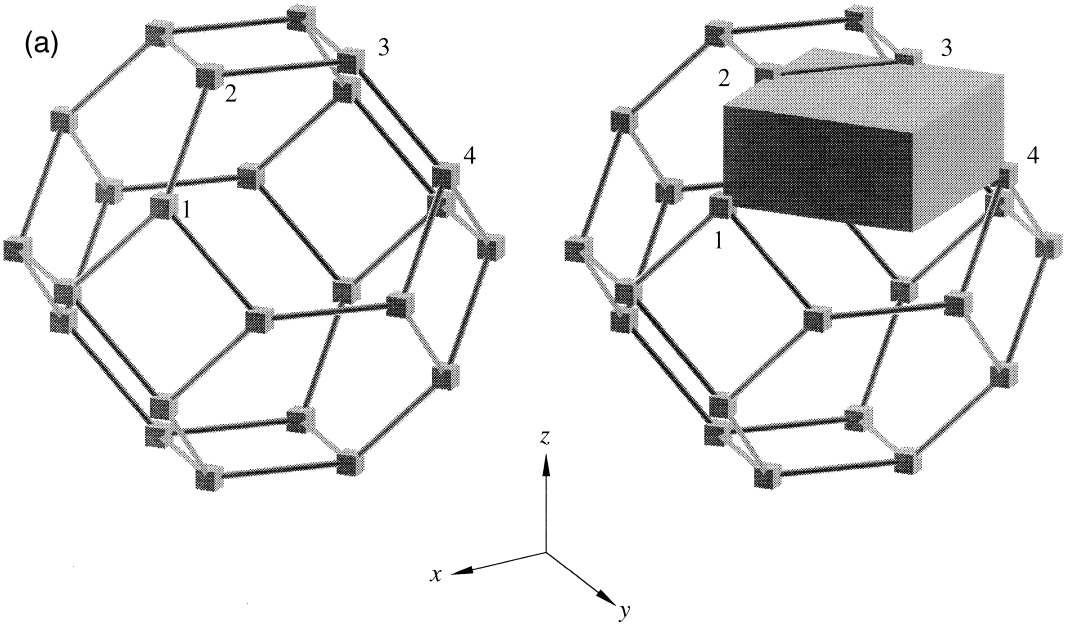

Fig. 1. (a) The tetrakaidecahedron modeled with cylindrical ligaments and cubic nodes. The Cartesian coordinate system is shown for the clarification of the projected unit cell displayed in (b). The labeled nodes (1–4) correspond to the respective nodes labeled in (b). The unit cell is shown on the right as a solid block located in a single tetrakaidecahedron cell. (b) The geometrical breakdown of the unit cell of the tetrakaidecahedron. The thick lines denote the solid surfaces within the unit cell. Points 1–4 correspond with (a) to describe the projection onto the y–z plane. (c) Single tetrakaidecahedron cell in an aluminum foam.

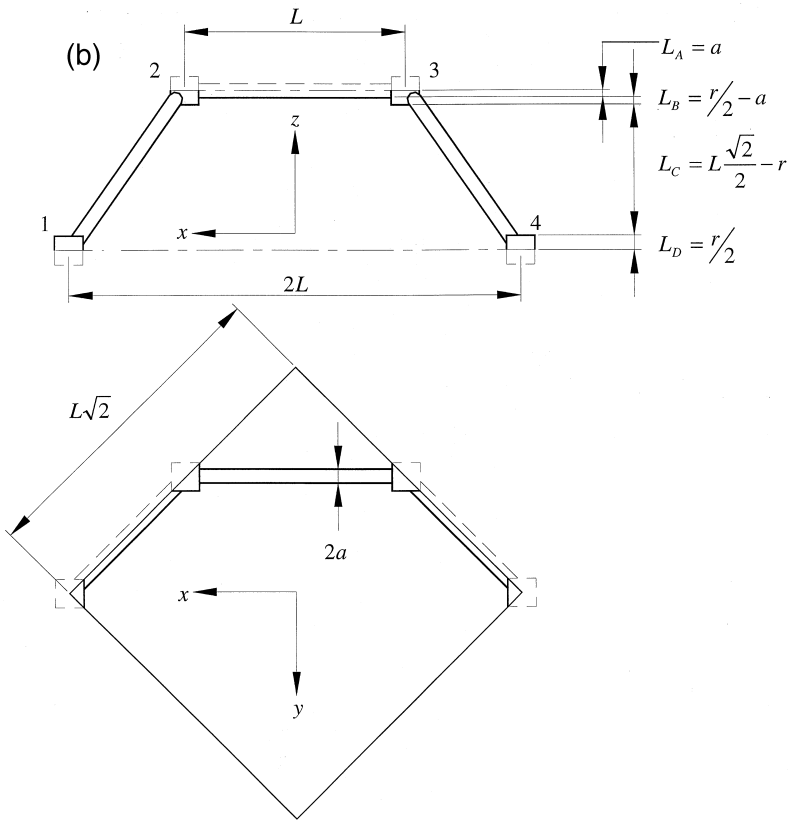

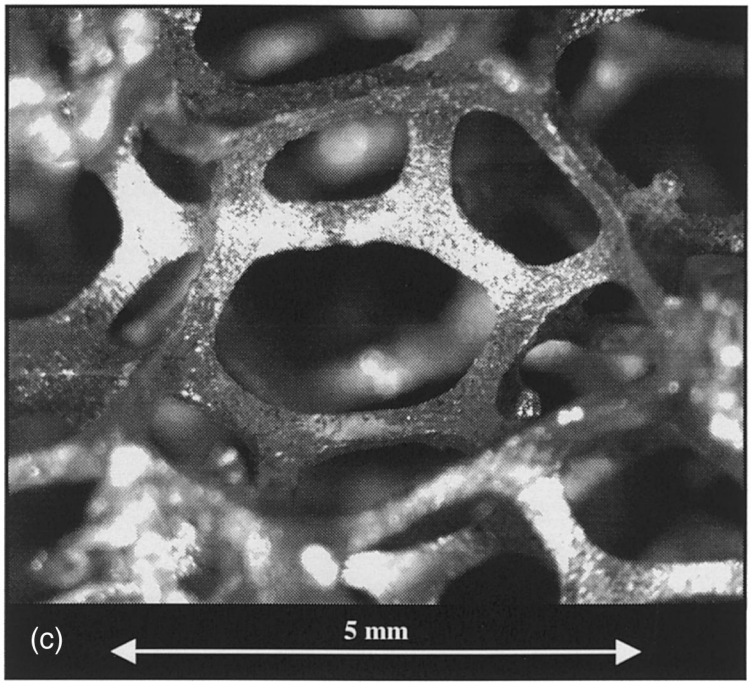

Fig. 1 (*continued*)

losophical Magazine in 1887 by Lord Kelvin [1]. The tetrakaidecahedron is the idealized shape that will most likely be attained in the foam from the nature of the foaming process [18]. When the aluminum is in its molten state during manufacturing, foaming gas is injected into the molten slurry causing bubble formation. These gas bubbles are free to move around and pack themselves into a given space following a tendency to attain a natural state of lowest surface energy, while the liquid accumulates at the edges of the bubbles, forming the final foam structure. The actual components of the foam network were represented geometrically in the three-dimensional model by cubical nodes and cylindrical ligaments. The length of the cubic node was denoted by r, while the ligament was defined by its length, L, and the radius of its cross section, a (Fig. 1b). A magnified tetrakaidecahedron photographed from a real aluminum foam is shown in Fig. 1c.

3. Model development

3.1. Porosity

Taking the cells in their connected state, a representative section was selected based on symmetry. This encapsulates one sixteenth of a single tetrakaidecahedron cell (Fig. 1b). This representative section contains all the geometrical characteristics relating to the tetrakaidecahedron. In this section, discrete layers were defined based on distinct geometrical features. The height of the rectangular unit cell in the z direction (Fig. 1b) is

$$L\frac{\sqrt{2}}{2} \tag{2}$$

with the two other sides of the rectangular unit cell in the x–y plane being

$$L\sqrt{2} \tag{3}$$

where L is the length between node centers in the tetrakaidecahedron. Two other variables (a and r) break up the unit cell into four distinct vertical layers (Fig. 1b). From the top with respect to the z axis, the height for the first section, A, is a, because half of the cylindrical ligament belongs to the unit cell and the other half to the cell located above it. Proceeding downwards to section B, the next descriptive height is the quantity $r/2-a$, described by the difference between half the node side length and the ligament radius. Moving directly to the bottom section D, the height is simply represented by half the side length of the cubic node, $r/2$. The height for the final section C is given by the difference of the remaining height and the total unit cell's height projected onto the y–z plane (Eq. (2)).

$$L\frac{\sqrt{2}}{2} - r \tag{4}$$

Having the heights defined for these four sections, the total volume for each rectangular section is calculated simply by multiplying the unit cell's area in the x–y plane by the z height of the individual sections (A, B, C, D) to give the following volumes.

$$V_{\mathrm{A}} = 2aL^2 \tag{5}$$

$$V_{\mathrm{B}} = (r-2a)L^2 \tag{6}$$

$$V_{\mathrm{C}} = 2\left(\frac{1}{2}L\sqrt{2} - r\right)L^2 \tag{7}$$

$$V_{\mathrm{D}} = rL^2 \tag{8}$$

A simplification can be made by using the following non-dimensional relationships.

$$d = \frac{a}{L} \tag{9}$$

$$e = \frac{r}{L} \tag{10}$$

The next step is calculating the volume occupied by the solid for each layer using the dimensionless d and e variables.

$$V_{\mathrm{A,s}} = \left(e^2 + \frac{1}{2}d\pi(1-e)\right)dL^3 \tag{11}$$

$$V_{\mathrm{B,s}} = \left(\frac{1}{2}e - d\right)e^2L^3 \tag{12}$$

$$V_{\mathrm{C,s}} = \left(1-2e\sqrt{2}\right)\pi d^{\,2}L^3 \tag{13}$$

$$V_{\mathrm{D,s}} = \frac{1}{4}e^3L^3 \tag{14}$$

Having these relationships, the porosity can be estimated on the basis of d and e.

$$\varepsilon = 1 - \frac{\sqrt{2}}{2}\left(de^2 + \frac{1}{2}\pi d^{\,2}(1-e) + \left(\frac{1}{2}e - d\right)e^2 + \pi d^{\,2}\left(1-2e\sqrt{2}\right) + \frac{1}{4}e^3\right) \tag{15}$$

The variables e and d need to be eliminated to obtain the ultimate goal, the effective thermal conductivity as a function of the material properties and the porosity. Solving Eq. (15) for an arbitrary porosity, ε, yields a quadratic solution for d, which is used later for the effective thermal conductivity.

$$d = \sqrt{\frac{\sqrt{2}\left(2 - (5/8)e^3\sqrt{2} - 2\varepsilon\right)}{\pi\left(3 - 4e\sqrt{2} - e\right)}} \tag{16}$$

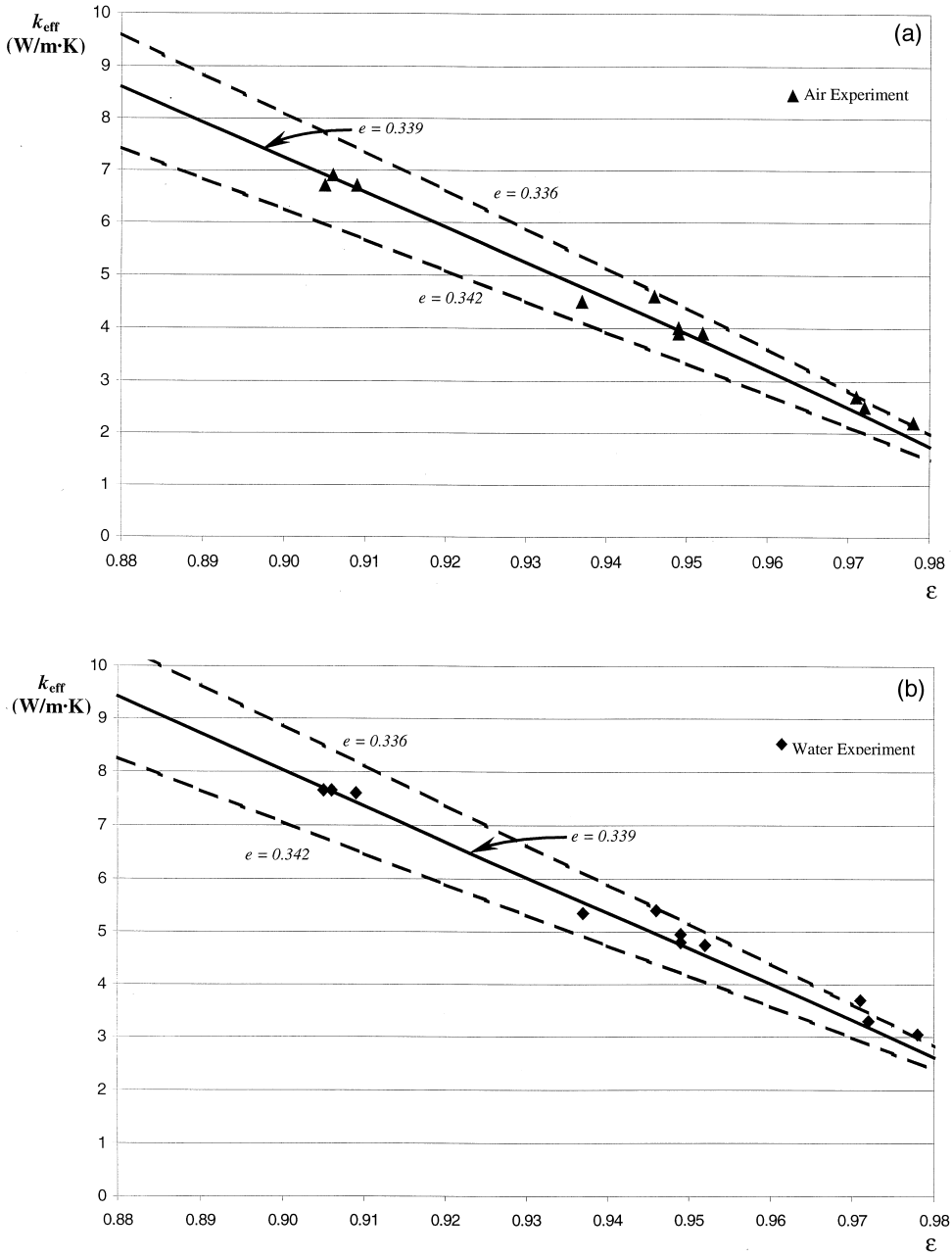

Fig. 2. Plot of k_{eff} for various porosities and dimensionless e values for calibration of the three-dimensional model with air against experimental data [2]. The solid line represents the e value chosen from the calibration procedure. (b) Plot of k_{eff} for various porosities and dimensionless e values for calibration of the three-dimensional model with water against experimental data [2]. The solid line represents the e value chosen from the calibration procedure.

3.2. Thermal conductivity

Averaging the thermal conductivity of each section on the basis of the individual volume fractions and their respective thermal conductivities is done in the following manner, as in Eq. (1).

$$k_n = \frac{V_{n,s}k_s + (V_n - V_{n,s})k_f}{V_n} \tag{17}$$

This thermal conductivity is calculated for each section (n = A, B, C, D). The thermal conductivity through the representative section is calculated based on heat conduction through a series of four levels using Fourier's law of heat conduction to give the relation.

$$k_{eff} = \frac{L_A + L_B + L_C + L_D}{(L_A/k_A) + (L_B/k_B) + (L_C/k_C) + (L_D/k_D)} \tag{18}$$

Substituting the equations for the section lengths (L_n), the thermal conductivities for each (k_n), and the positive solution for d from Eq. (16) yields a lengthy equation for the effective thermal conductivity as a function of the porosity, e, and d (which is a solved function of ε and e from Eq. (15)). Introducing the simplifying notation

$$R_A = \frac{4d}{(2e^2 + \pi d(1-e))k_s + (4 - 2e^2 - \pi d(1-e))k_f} \tag{19}$$

$$R_B = \frac{(e-2d)^2}{(e-2d)e^2k_s + (2e - 4d - (e-2d)e^2)k_f} \tag{20}$$

$$R_C = \frac{\left(\sqrt{2} - 2e\right)^2}{2\pi d^2\left(1 - 2e\sqrt{2}\right)k_s + 2\left(\sqrt{2} - 2e - \pi d^2\left(1 - 2e\sqrt{2}\right)\right)k_f} \tag{21}$$

$$R_D = \frac{2e}{e^2k_s + (4 - e^2)k_f} \tag{22}$$

finally yields the final result of the effective thermal conductivity to be

$$k_{eff} = \frac{\sqrt{2}}{2(R_A + R_B + R_C + R_D)} \tag{23}$$

4. Results and discussion

This k_{eff} function is plotted for two separate cases. Aluminum (k = 218 W m^{-1} K^{-1}) is used for the solid in both cases. In Fig. 2a, air (k = 0.0265 W m^{-1} K^{-1}) is the saturating fluid, and in Fig. 2b, water (k = 0.613 W m^{-1} K^{-1}) is the saturating fluid. The e value is calibrated from these figures by comparison of the model calculations against the experimental data from Calmidi and Mahajan [2]. The reason why this process was selected was to assure a reasonable balance between the node and ligament sizes and to investigate the thermal conductivity dependence on the changes in the relative thickness of the ligaments.

Examining Fig. 2a shows that the best agreement between the variable e and the available experimental data for porous aluminum saturated with air is for e = 0.339. This effective geometrical ratio carries over for the water saturated aluminum medium as well, as shown by Fig. 2b.

The ratio of the effective thermal conductivity to the fluid conductivity is calculated and plotted in Fig. 3 for several relationships of k_s/k_f and porosity using the value e = 0.339. The calculated effective thermal conductivity ratio by the phase-symmetry model of Hsu et al. [12] is also plotted on the same graph as dashed lines for comparison.

The effect of the fluid conductivity at relatively high porosities ($\varepsilon \sim 0.95$) on the effective thermal conductivity of the saturated porous medium is of interest because it aids the selection of the best fluid/solid combination. In Fig. 4, the effective thermal conductivity for a fluid saturated porous aluminum matrix of 95% porosity is plotted for a wide range of fluid conductivities from 0.0 to 10.0 W m^{-1} K^{-1}.

Comparing the three-dimensional model to the experimental data shows that the model follows the curve of the data points very well in both cases with air and water as the saturating fluids. The calibration curves that were done for air and water lie directly on the data points taken from Calmidi and Mahajan [2]. In both cases the closest (and very good) relationship between the experimental and calculated points, as shown in Fig. 2b, was achieved for a value of e = 0.339. These results are compared with the values obtained using the phase-symmetry model developed by Hsu et al. [12] which are also plotted in Fig. 3 as dashed lines for various values of k_s/k_f and the air and water values. The present three-dimensional geometric model predicts a lower effective thermal conductivity than the phase-symmetry model throughout the plotted porosity range for realistic metal to saturating fluid conductivity ratios and solid matrix porosities ($\varepsilon <$ 0.98), and agrees everywhere with the experiments. At a lower phase conductivity ratio of $k_s/k_f = 100$, the present three-dimensional model predicts a lower effective thermal conductivity at porosities lower than $\varepsilon = 0.965$. For $k_s/k_f = 10$ the present model predicts a higher thermal conductivity than the phase-symmetry model

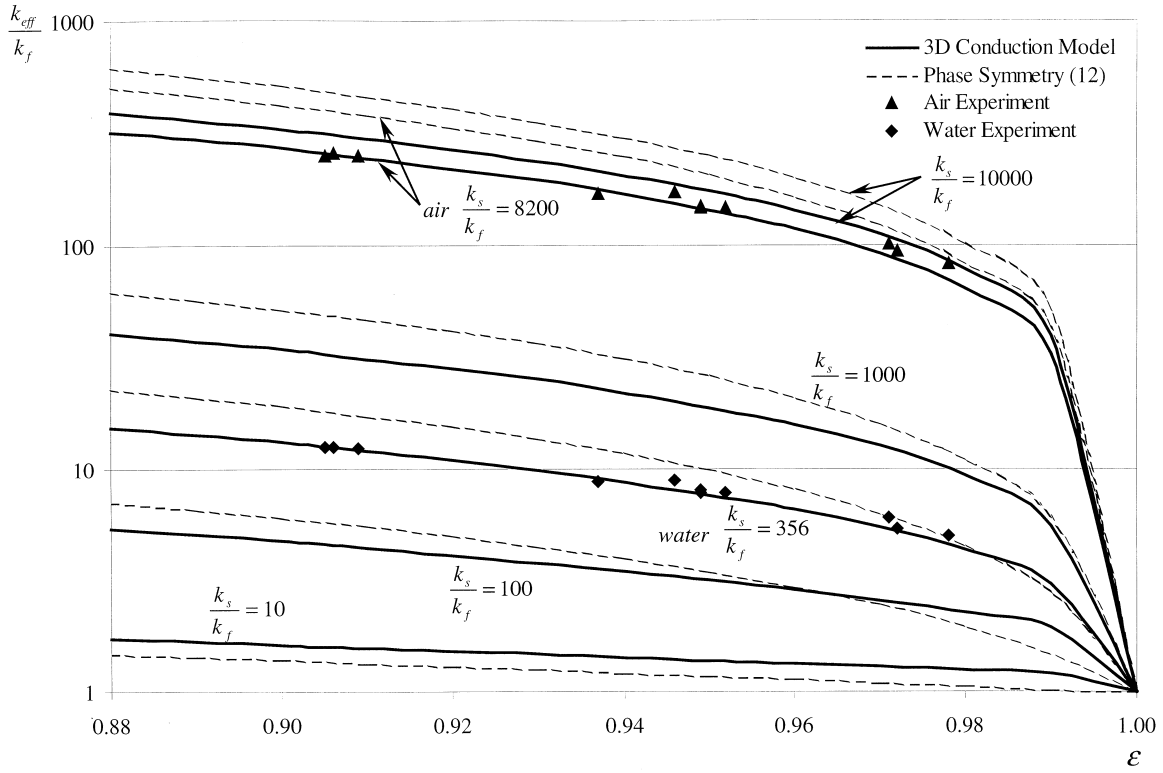

Fig. 3. Plot of the dimensionless thermal conductivities for the three-dimensional model with $e = 0.339$ and the phase-symmetry model by Hsu et al. [12] for various k_s/k_f values plus the air and water cases which are compared to experimental data points [2].

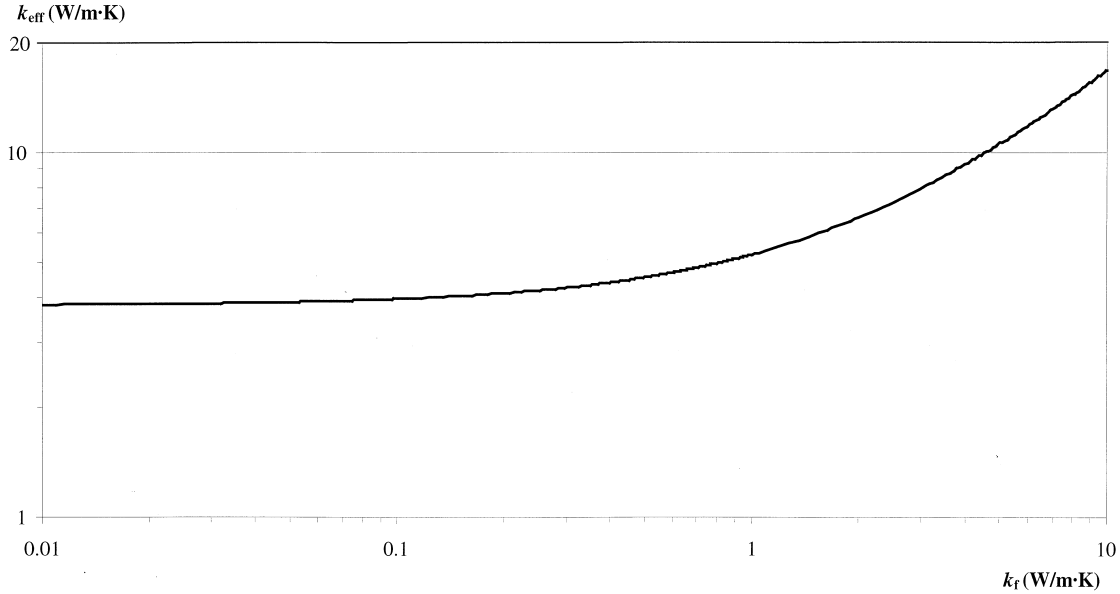

Fig. 4. Effective thermal conductivity for a saturated porous aluminum medium ($k = 218$ W m^{-1} K^{-1}, $\varepsilon = 0.95$) by varying the fluid conductivity (k_f).

across the entire porosity range shown, from $\varepsilon = 0.88$ to 1.00.

It is useful to observe the effects on the effective thermal conductivity while varying the fluid conductivity in order to find an optimal solid–fluid system. In Fig. 4 the effective thermal conductivity for a saturated aluminum matrix of $\varepsilon = 0.95$ is plotted with varying k_f from 0.0 to 10.0 W m^{-1} K^{-1}. Following the plot where there is nearly a vacuum ($k_f = 0.01$ W m^{-1} K^{-1}) to a $k_f = 0.1$ W m^{-1} K^{-1} shows a nearly negligible increase in the effective thermal conductivity, from 3.82 to 3.95 W m^{-1} K^{-1}, or a 3% increase in k_{eff} for an order of magnitude increase in k_f. Proceeding another order of magnitude to a thermal conductivity value of $k_f = 1.0$ W m^{-1} K^{-1} shows a larger change in the effective thermal conductivity from 3.95 to 5.24 W m^{-1} K^{-1}, or an increase of 33%. Continuing to increase the fluid conductivity all the way to $k_f = 10.0$ W m^{-1} K^{-1} shows a relatively large increase in effective thermal conductivity to 16.7 W m^{-1} K^{-1}, or an increase of 220% in k_{eff} for an increase in fluid conductivity of one order of magnitude. However, only non-conventional fluids, such as liquid mercury, possess such a thermal conductivity. Restricting the discussion to practical fluids like water or ethylene glycol where $k_f < 1.0$ W m^{-1} K^{-1}, these changes in effective thermal conductivity values reveal that relatively minimal gains are made in increasing k_{eff} when the solid to fluid conductivity ratio is high. Increasing the thermal conductivity of the solid phase is required for any dramatic improvement in the effective thermal conductivity of the composite system.

5. Conclusion

A one-dimensional heat conduction model for use with open celled metallic foams was developed based on a three-dimensional description of the foam geometry. This detailed description of the foam geometry allows the effective thermal conductivity to be calculated accurately. The three-dimensional model fits the experimental data [2] very well and performs better than the phase-symmetry model for the parameter ranges typically experienced in metal foams. Because of the accurate curve prediction, this model may lend itself well into applicability in the lower porosity regimes ($\varepsilon < 0.90$).

The three-dimensional model demonstrated that for metal foams in which the solid conductivity is markedly higher than the fluid conductivity improvements in the overall effective thermal conductivity are best made by increasing the thermal conductivity of the solid phase through manipulation of the foam solid structure at the manufacturing phase, since the solid phase appears to govern the effective thermal conductivity value, even at a very high porosity.

Acknowledgements

It is gratefully acknowledged that this research was supported jointly by the Swiss Commission for Technology and Innovation (CTI) through project no. 4150.2 and by the ABB Corporate Research Center, Baden-Daettwil, Switzerland. Helpful discussions with Dr Alexander Stuck and Dr Fabian Zwick of the ABB Corporate Research Center during the course of the work are also acknowledged.

References

[1] W. Thomson, On the division of space with minimum partitional area, Phil. Mag. 5 (24) (1887) 503–514.
[2] V.V. Calmidi, R.L. Mahajan, The effective thermal conductivity of high porosity fibrous metal foams, J. Heat Transfer 121 (1999) 466–471.
[3] J.C. Maxwell, in: A Treatise on Electricity and Magnetism, Clarendon Press, Oxford, 1873, p. 365.
[4] Lord Rayleigh, On the influence of obstacles arranged in rectangular order upon the properties of a medium, Phil. Mag. L VI (1892) 481–502.
[5] K.J. Renken, D.P. Poulikakos, Experiment and analysis of forced convective heat transport in a packed bed of spheres, Int. J. Heat Mass Transfer 31 (7) (1988) 1399–1408.
[6] K.J. Renken, D.P. Poulikakos, Experiments on forced convection from a horizontal heated plate in a packed bed of glass spheres, Phys. Fluids 28 (12) (1985) 3477–3484.
[7] D.P. Poulikakos, K.J. Renken, Forced convection in a channel filled with porous medium, including the effects of flow inertia, variable porosity, and Brinkman friction, J. Heat Transfer 109 (1987) 880–888.
[8] B.V. Antohe, J.L. Lage, D.C. Price, R.M. Weber, Numerical characterization of micro heat exchangers using experimentally tested porous aluminum layers, Int. J. Heat Fluid Flow 17 (1996) 594–603.
[9] M.L. Hunt, C.L. Tien, Effects of thermal dispersion on forced convection in fibrous media, Int. J. Heat Mass Transfer 31 (2) (1988) 301–309.
[10] C.L. Tien, K. Vafai, Statistical bounds for the effective thermal conductivity of microsphere and fibrous insulation, Prog. Astronaut. Aeronaut. 65 (1979) 135–148.
[11] B.V. Antohe, J.L. Lage, D.C. Price, R.M. Weber, Numerical characterization of micro heat exchangers using experimentally tested porous aluminum layers, Int. J. Heat Fluid Flow 17 (1996) 594–603.
[12] C.T. Hsu, P. Cheng, K.W. Wong, Modified Zehner–Schlunder models for stagnant thermal conductivity of porous media, Int. J. Heat Mass Transfer 37 (17) (1994) 2751–2759.
[13] P. Zehner, E.U. Schlunder, Thermal conductivity of

granular materials at moderate temperatures, Chem. Ing. -Tech. 42 (1970) 933–941.
[14] C.L. Tien, M.L. Hunt, Boundary-layer flow and heat transfer in porous beds, Chem. Eng. Process 21 (1987) 53–63.
[15] S. Whitaker, The Method of Volume Averaging, Kluwer Academic Publishers, Dordrecht, The Netherlands, 1999, p. 80.
[16] A. Amiri, K. Vafai, Analysis of dispersion effects and non-thermal equilibrium, non-Darcian, variable porosity incompressible flow through porous media, Int. J. Heat Mass Transfer 37 (6) (1994) 939–954.
[17] M. Kaviany, Principles of Heat Transfer in Porous Media, Springer, New York, 1995, p. 119.
[18] D'Arcy Thompson, On Growth and Form, Canto, Cambridge, 1995, p. 121.